

**Simulating the last glacial termination**

M. Heinemann et al.

This discussion paper is/has been under review for the journal *Climate of the Past* (CP). Please refer to the corresponding final paper in CP if available.

# Deglacial ice–sheet meltdown: orbital pacemaking and CO<sub>2</sub> effects

M. Heinemann<sup>1</sup>, A. Timmermann<sup>1,2</sup>, O. E. Timm<sup>3</sup>, F. Saito<sup>4</sup>, and A. Abe-Ouchi<sup>4,5</sup>

<sup>1</sup>International Pacific Research Center, School of Ocean and Earth Science and Technology, University of Hawaii, Honolulu, USA

<sup>2</sup>Department of Oceanography, School of Ocean and Earth Science and Technology, University of Hawaii, Honolulu, USA

<sup>3</sup>Department of Atmospheric and Environmental Sciences, University at Albany, State University of New York, Albany, USA

<sup>4</sup>Research Institute for Global Change, Japan Agency for Marine–Earth Science and Technology, Yokohama, Japan

<sup>5</sup>Atmosphere Ocean Research Institute, University of Tokyo, Kashiwa, Japan

Received: 8 January 2014 – Accepted: 24 January 2014 – Published: 5 February 2014

Correspondence to: M. Heinemann (malteh@hawaii.edu)

Published by Copernicus Publications on behalf of the European Geosciences Union.

[Title Page](#)

[Abstract](#)

[Introduction](#)

[Conclusions](#)

[References](#)

[Tables](#)

[Figures](#)

[I ◀](#)

[▶ I](#)

[◀](#)

[▶](#)

[Back](#)

[Close](#)

[Full Screen / Esc](#)

[Printer-friendly Version](#)

[Interactive Discussion](#)



## Abstract

Eighty thousand years of ice-sheet build-up came to a rapid end ~20–10 thousand years before present (ka BP), when ice sheets receded quickly, and global mean surface temperatures rose by about 4°C. It still remains unresolved whether insolation changes due to variations of earth's tilt and orbit were sufficient to terminate glacial conditions. Using a coupled three-dimensional climate–ice-sheet model, we simulate the climate and Northern Hemisphere ice-sheet evolution from 78 to 0 ka BP in good agreement with sea level and ice topography reconstructions. Based on this simulation and a series of deglacial sensitivity experiments with individually varying orbital parameters and CO<sub>2</sub>, we find that enhanced calving led to a slow-down of ice-sheet growth already 5 to 8 ka prior to the Last Glacial Maximum (LGM), as evidenced by the change in curvature of the simulated and reconstructed ice volume time series. Increasing obliquity and precession then led to accelerated ice loss due to ablation and calving, thereby initiating the glacial termination. The deglacial sensitivity experiments further reveal that the ~ 100 ppmv rise of atmospheric CO<sub>2</sub> after ~ 18 ka BP was a key contributor to the deglaciation. Without it, the present-day ice volume would be comparable to that of the LGM and global mean temperatures would be about 3°C lower than today. We further demonstrate that neither orbital forcing nor CO<sub>2</sub> forcing alone were sufficient to complete the deglaciation.

## 1 Introduction

The last glacial termination (20–10 ka BP) is a well-documented period of global climate reorganization and ice-sheet retreat with extensive paleo-data coverage (Waelbroeck et al., 2002; Peltier and Fairbanks, 2006; Yokoyama and Esat, 2011; Clark et al., 2012; Shakun et al., 2012). It provides an optimal test bed to study the combined effects of orbital forcing (Milankovitch, 1941; Berger, 1978) and greenhouse gas (GHG) feedbacks onto the climate system. Whereas previous modeling studies (Gallée et al.,

CPD

10, 509–532, 2014

## Simulating the last glacial termination

M. Heinemann et al.

Title Page

Abstract

Introduction

Conclusions

References

Tables

Figures

◀

▶

◀

▶

Back

Close

Full Screen / Esc

Printer-friendly Version

Interactive Discussion



## Simulating the last glacial termination

M. Heinemann et al.

Title Page

Abstract

Introduction

Conclusions

References

Tables

Figures

◀

▶

◀

▶

Back

Close

Full Screen / Esc

Printer-friendly Version

Interactive Discussion



1992; Yoshimori et al., 2001; Ganopolski and Calov, 2011; Abe-Ouchi et al., 2013) have identified GHG variations as a contributor to Pleistocene Northern Hemisphere ice-sheet variability, their role in triggering and promoting the deglacial retreat of the Laurentide, Greenland and Eurasian ice sheets during the last glacial termination has not been firmly established. In this study we determine the transient effects of orbital and greenhouse gas changes during the last deglaciation using a 3 dimensional coupled climate–ice-sheet model.

Our study augments a multitude of recent transient modeling studies (Timm and Timmermann, 2007; Timmermann et al., 2009; Ganopolski and Roche, 2009; Roche et al., 2011; Smith and Gregory, 2012; He et al., 2013) that focus on the effects of orbital forcing, GHG, and ice-sheet changes on the deglacial evolution of the atmosphere–ocean system. In these numerical experiments, however, the ice-sheet evolution was not interactively calculated, but rather prescribed. Hence key glacial climate feedbacks onto the ice-sheet, such as the elevation–desert effect (Yamagishi et al., 2005), ice albedo and stationary wave feedbacks (Roe and Lindzen, 2001; Abe-Ouchi et al., 2013), and ocean–cryosphere interactions (Gildor and Tziperman, 2000) were not represented. To quantify the importance of such feedbacks for glacial cycle dynamics, climate–ice-sheet models of varying complexity have been employed, including zero-dimensional conceptual models (Källén et al., 1979), box models (Gildor and Tziperman, 2000), two-dimensional zonally averaged coupled climate–ice-sheet models (Gallée et al., 1992), three-dimensional ice-sheet models driven by climatic parameterizations derived from atmosphere–ocean general circulation models (Abe-Ouchi et al., 2007, 2013), and three-dimensional ice-sheet models coupled to earth system models of intermediate complexity (Ganopolski and Calov, 2011).

Section 2 describes the set-up and coupling strategy of the intermediate complexity coupled ice-sheet–climate model iLove and the configuration of the deglacial sensitivity experiments. The model spin-up is described in Sect. 3. In Sect. 4, the main results of our transient modeling experiments are presented. This section includes a description of the overall performance of the coupled model, an analysis of ice-sheet mass balance

changes, and sensitivity studies with respect to orbital parameters and CO<sub>2</sub>. The paper concludes with a discussion of the main results and uncertainties.

## 2 Ice-sheet – climate model setup

The numerical model used in this study, hereafter called iLove, is based on the ice-sheet model for Integrated Earth system Studies IclES (Saito and Abe-Ouchi, 2004; Abe-Ouchi et al., 2007), bi-directionally coupled to the atmosphere-ocean-sea ice-land components of the intermediate complexity model LOVECLIM 1.0 (Driesschaert et al., 2007). The coupled model is driven by orbital parameter changes (Berger, 1978), and reconstructed atmospheric concentrations of CO<sub>2</sub> (Lüthi et al., 2008), CH<sub>4</sub> (Loulergue et al., 2008), and N<sub>2</sub>O (Schilt et al., 2010).

IclES applies the shallow ice approximation to compute the thickness and temperature evolution of grounded ice. Floating ice shelves are not accounted for. Here, IclES is set up to simulate land ice north of 30° N on a 1° by 1° spherical grid. The surface mass balance is approximated by a positive-degree-day (PDD) scheme. Bedrock elevation is computed dynamically assuming local isostatic rebound (mantle density of 4500 kg m<sup>-3</sup>, time scale 5000 yr). For simplicity, a fixed grounding line is used (Fig. 1b). In addition to the passive calving at the grounding line, a parameterization of active calving into proglacial lakes is applied. IclES sensitivity runs for the last four glacial cycles with respect to this active calving parameterization, mantle density and time scale for isostatic rebound were described in a previous study (Abe-Ouchi et al., 2013).

LOVECLIM is based on the quasi-geostrophic atmosphere model ECBilt (Opsteegh et al., 1998) with ageostrophic correction terms, 3 vertical levels and T21 spectral truncation, corresponding to a horizontal grid-spacing of ~ 5.6°. The effect of carbon dioxide (CO<sub>2</sub>), methane (CH<sub>4</sub>), and nitrous oxide (N<sub>2</sub>O) on the longwave radiation is computed with a radiation scheme that is linearized around reference profiles (Schaeffer et al., 1999; Goosse et al., 2010). Here, to account for the low sensitivity of ECBilt to CO<sub>2</sub> variations, the effect of CO<sub>2</sub> deviations from the reference value of 356 ppmv on the

CPD

10, 509–532, 2014

## Simulating the last glacial termination

M. Heinemann et al.

Title Page

Abstract

Introduction

Conclusions

References

Tables

Figures

◀

▶

◀

▶

Back

Close

Full Screen / Esc

Printer-friendly Version

Interactive Discussion



longwave flux is scaled (Timm and Timmermann, 2007) by a factor of  $\alpha = 3$ . With this scaling factor, the present-day equilibrium climate sensitivity of iLove (including the Greenland ice-sheet response) to CO<sub>2</sub> doubling amounts to about 4 °C. The importance and drawbacks of this scaling are discussed in Sect. 5.

5 The ocean-sea ice component of LOVECLIM, CLIO (Goosse and Fichefet, 1999, Coupled Large-scale Ice Ocean), computes ocean currents, salinity, and temperature according to the primitive equations on two spherical sub-grids covering the global oceans at a resolution of 3° by 3° horizontally, and 20 levels vertically; sea ice thermodynamics and advection are computed on the same horizontal grid. The terrestrial biosphere component of LOVECLIM, VECODE (Brovkin et al., 1999, VEgetation COntinuous DEscription), assigns tree, grass, and desert fractions to land points not covered by ice.

10 Coupling between LOVECLIM and IclES is accomplished by the asynchronous exchange of orography, albedo, forest fraction, surface temperatures, and precipitation. The faster-responding atmosphere–ocean–sea-ice–vegetation components are subject to accelerated GHG and orbital forcings (Timm and Timmermann, 2007), by a factor of 20, while the land ice component has real time to adjust to the corresponding climate anomalies. Every 1000 forcing years, equivalent to 50 model years in LOVECLIM, climatologies of monthly mean surface temperature, and precipitation are passed to IclES to drive the surface mass balance computations. The surface temperature is corrected for its present-day bias before it is passed onto IclES. It should be noted here that the LOVECLIM surface temperature warm bias over North America is quite substantial (up to 7 °C, Fig. 1a) and needs to be subtracted to allow IclES to build a realistic ice sheet. LOVECLIM in turn receives the current surface elevation and ice extent to update the orography, surface albedo, and forest fraction. Ice-ocean freshwater and heat exchange are not accounted for in our model setup.

## Simulating the last glacial termination

M. Heinemann et al.

[Title Page](#)[Abstract](#)[Introduction](#)[Conclusions](#)[References](#)[Tables](#)[Figures](#)[I ◀](#)[▶ I](#)[◀](#)[▶](#)[Back](#)[Close](#)[Full Screen / Esc](#)[Printer-friendly Version](#)[Interactive Discussion](#)

### 3 Model spin-up

To achieve a realistic transient simulation of the Last Glacial Maximum (LGM), a two-step initialization approach is pursued. First, the model is initialized for the Eemian interglacial at 125 kaBP (Fig. 1c) using present-day climate and ice-sheet initial conditions. However, in this transient simulation the glacial inception is not captured well; sizeable ice sheets only build up after 70 kaBP, in contrast to paleo-climate records, which show an early glacial inception around 115 ka BP. Moreover, it appears that the ice sheets do not reach the critical extent necessary to persist through the phase of large precession and obliquity at the start of marine isotope stage 3 (MIS 3, see Fig. 2c and d for orbital and CO<sub>2</sub> forcings). A possible reason for this late and weak inception is the low spatial resolution of our atmosphere component ECBilt (T21), which ignores small-scale topographic features that may have played an important role in the initial glacial ice-sheet build-up (Abe-Ouchi and Blatter, 1993; Pollard and Thompson, 1997; Calov et al., 2005). The simulated ice volume in the first iteration at 63 kaBP is similar to the reconstructed global ice volume (sea level) at 78 kaBP. Hence, in a second iteration, the simulation is restarted at 78 kaBP using the ice sheet state from the initial run at 63 kaBP (Fig. 1c, blue lines). This second step leads to an improved glacial build up of ice during MIS 3, avoiding the unrealistic deglaciation that occurred in the initial iteration. The strong sensitivity of the glacial trajectory to the initial conditions indicates the presence of multiple equilibria for MIS 3 boundary conditions.

### 4 Modeling results

#### 4.1 The transient evolution of iLove over the past 78 ka

Given large enough ice sheets prior to MIS 3, the evolution of the Northern Hemisphere ice sheets as simulated in the control run (CTR) with prescribed time-varying GHG and orbital forcing is in good agreement with sea level proxies (Waelbroeck et al., 2002;

## Simulating the last glacial termination

M. Heinemann et al.

Title Page

Abstract

Introduction

Conclusions

References

Tables

Figures

◀

▶

◀

▶

Back

Close

Full Screen / Esc

Printer-friendly Version

Interactive Discussion



## Simulating the last glacial termination

M. Heinemann et al.

Title Page

Abstract

Introduction

Conclusions

References

Tables

Figures

◀

▶

◀

▶

Back

Close

Full Screen / Esc

Printer-friendly Version

Interactive Discussion



Peltier, 2004; Yokoyama and Esat, 2011) and ice sheet reconstructions (Peltier, 2004) during the subsequent glacial ice sheet build-up, the LGM, the deglaciation, and the Holocene (Figs. 2a and 3). Furthermore, CTR simulates a relatively stable Greenland ice-sheet across the glacial termination and into the Holocene, in accordance with observations (Fig. 3).

Comparing the deglacial evolution of the simulated ice sheets with the ICE-5G paleotopographic reconstruction (Peltier, 2004, Figs. 2a and 3a–f), we find good agreement, in particular for the retreat of the Laurentide ice-sheet. On its deglacial retreat, the Laurentide ice sheet passes Lake Winnipeg and the Great Slave Lake in northwestern Canada around 10 kaBP. During this progression the Laurentide ice sheet undergoes a saddle collapse (also called “zipper-effect”), a separation of the Cordilleran and Labrador/Keewatin ice sheets at around 11 kaBP (Fig. 3e), similar to previous modeling results obtained with off-line ice sheet models (Gregoire et al., 2012; Abe-Ouchi et al., 2013). For the LGM, the simulation and reconstruction of the Laurentide ice sheet differ over Alaska and the Aleutian Islands, and the Laurentide ice sheet dome is further eastward in iLove. The Greenland and Laurentide ice sheets are thicker towards the margins, which leads to an overestimation of the LGM global ice volume in CTR by about 20 m sea-level equivalent (sle, Fig. 2a). The simulated Eurasian LGM ice sheet is smaller than the reconstruction and lacks ice cover over the Baltic Sea and the Barents and Laptev Seas, Central Europe and the British Isles. It should be noted here that the prescribed grounding line mask (Fig. 1b) prevented the Eurasian ice sheet from spreading across the North Sea and into the British Isles. This unrealistic feature will be corrected in future experiments with iLove.

### 4.2 Orbital and CO<sub>2</sub> effects

To elucidate the individual roles of atmospheric CO<sub>2</sub> changes and orbital forcing during the deglaciation, two transient sensitivity experiments are performed using LGM (21 kaBP) initial conditions from the iLove CTR experiment. In the first experiment, the atmospheric GHG concentrations are kept constant at LGM values, and only the orbital

## Simulating the last glacial termination

M. Heinemann et al.

Title Page

Abstract

Introduction

Conclusions

References

Tables

Figures

◀

▶

◀

▶

Back

Close

Full Screen / Esc

Printer-friendly Version

Interactive Discussion



5 forcing is varied from 21 kaBP to today (Fig. 2a, blue line). Initially, the corresponding Northern Hemisphere ice volume decreases until about 9 kaBP, with a similar onset of the deglaciation compared to CTR. However, in response to the switch from a warm to a cold orbit with decreasing obliquity and summer insolation, the ice sheets start to recover. This experiment documents that direct orbital forcing alone was not sufficient to complete the deglaciation. Hence, the observed increase of CO<sub>2</sub> between 18 kaBP to about 9 kaBP was an essential element for the ice sheet retreat during the last glacial termination. If atmospheric CO<sub>2</sub> concentrations had remained at LGM values, large parts of North America would still be covered by thick ice sheets today (Fig. 3g).  
10 The second experiment, with fixed LGM orbital forcing and time-varying GHG concentrations (Fig. 2a, orange line) shows a 30–40 % deglacial ice sheet retreat, which is delayed by about 3 ka compared to CTR as a result of the late increase of atmospheric CO<sub>2</sub> concentrations starting around 18 kaBP. The fact that greenhouse gas changes alone are not sufficient for the deglaciation illustrates the importance of orbital forcing  
15 both for the timing and the amplitude of the last glacial termination. These sensitivity experiments make a compelling case for the importance of orbital and greenhouse gas forcing synergies as well as for the presence of nonlinearities in the coupled ice sheet/climate system that amplify the response to the combined forcing relative to the sum of the individual responses. A third experiment, starting at 40 kaBP with varying  
20 GHGs and obliquity but fixed precession, shows relatively small deviations from CTR (Fig. 2a, green line). This illustrates that, in our model, obliquity changes play a larger role for the timing of the LGM and the deglaciation than precessional variations.

### 4.3 Mass balance analysis

25 The evolution of the Northern Hemisphere ice sheet volume is determined by the time-integrated positive and negative ice sheet mass balance terms, namely accumulation, ablation, basal melting, and calving (Fig. 2b). For most of CTR from 78 kaBP until after the deglaciation at 10 kaBP, the total accumulation integrated over the ice sheets is proportional to the ice sheet area (dashed line in Fig. 2b). In other words, the mean

accumulation rate over the ice sheets remains almost constant. This supports the notion (Gallée et al., 1992; Yoshimori et al., 2001) that the growth and decay of the Northern Hemisphere ice sheets during this period are caused by variations of melting and calving, and not by variations of accumulation.

5 At the beginning of CTR, from 78 kaBP to about 60 kaBP, ablation, basal melting, and ice sheet calving are smaller than the accumulation rate, leading to a continuous growth of the ice volume from an initial value of about 40 m sle to about 90 m sle. Around 60 kaBP the combined effects of a high precessional index, which leads to shorter Northern Hemisphere summers and intensified peak insolation, increasing obliquity  
10 (Fig. 2d), and rising CO<sub>2</sub> concentrations (Fig. 2c) lead to a short reversal of the net mass balance and thus decreasing ice volume at the onset of marine isotope state 3 (MIS 3, 60–24 kaBP). In the subsequent period (50–32 kaBP), obliquity and precessional effects appear to almost cancel each other, resulting in a near neutral mass balance and hence slow ice sheet build-up. This lull is further promoted by the fact  
15 that atmospheric greenhouse gas concentrations stay relatively constant during MIS 3. At 32 kaBP, ice-sheet growth resumes. The Eurasian ice sheet starts to expand after it had mostly disappeared in our model simulation. During this time, the southern margin of the Laurentide ice sheet migrates southward, and the western margin into Alaska towards the Bering Strait. The larger ice sheet area leads to more accumulation  
20 (Fig. 2b). Slightly reduced calving and surface ablation rates further contribute to the larger net ice sheet growth ( $dV/dt$ ). The ice sheet area and mean accumulation rate keep rising until they peak at the LGM around 19 kaBP in our model. However,  $dV/dt$  already reaches its maximum around 28 kaBP, and subsequently decreases due to enhanced calving – despite the positive accumulation trend. This enhanced calving  
25  $\sim 5$ – $8$  ka prior to the LGM can be regarded as a precursor to the glacial termination. It is due to the fact that larger fractions of the expanding ice sheets reach their prescribed grounding line limits. Whether the amplified pre-LGM calving is linked to the obliquity rise at 28 kaBP remains unclear. Around 21 kaBP, ablation at the surface of the ice sheets intensifies, leading to a further reduction of  $dV/dt$ . At 19 kaBP,  $dV/dt$  eventually

CPD

10, 509–532, 2014

## Simulating the last glacial termination

M. Heinemann et al.

Title Page

Abstract

Introduction

Conclusions

References

Tables

Figures

◀

▶

◀

▶

Back

Close

Full Screen / Esc

Printer-friendly Version

Interactive Discussion



changes sign, which defines the LGM in our model and the beginning of the deglaciation. As described in Sect. 4.2, the rapidly magnified ablation that leads to the onset of the deglaciation is mostly caused by increasing obliquity, and is later enhanced by rising atmospheric CO<sub>2</sub>. During the subsequent Holocene period, a very stable Greenland ice sheet remains, for which accumulation, calving and ablation terms in the order of 0.05 Sv cancel each other almost completely.

#### 4.4 Global temperature changes during the deglaciation

The simulated global mean temperature rise during the deglaciation can be explained in large parts by rising CO<sub>2</sub> (Fig. 4a). In CTR, which includes both orbital forcing and GHG changes, the global mean temperature rise from 19 to 9 ka BP amounts to about 4 °C, which compares well with recent paleo-climate reconstructions (Shakun et al., 2012; Marcott et al., 2013). Note that, as mentioned in Shakun et al. (2012), the proxy data that form the basis for the reconstructed global mean temperature change are spatially biased towards ocean margins. Hence, the reconstructed amplitude of the global mean temperature change must be regarded with caution. Orbital forcing alone and its effect on surface albedo (causing a global reduction of 0.01, Fig. 4b), only account for about 0.5 °C, whereas the GHG changes alone are responsible for ~ 2.7 °C deglacial warming. Thus, the remaining temperature rise of 0.8 °C between 19–9 ka BP is due to synergy effects, characterising the nonlinear response of the coupled climate-ice sheet system to combinations of external forcings.

#### 4.5 Non-equilibrium LGM

Acknowledging the fact that ice sheets are integrators of mass imbalances, it is evident that they are typically not in equilibrium with external forcings on orbital timescales. The transient nature of the LGM ice sheet-climate system is further illustrated by branching off another sensitivity experiment from the LGM state of CTR with fixed LGM orbital and CO<sub>2</sub> forcings (Fig. 5). After about ninety thousand years of ice sheet integration

### Simulating the last glacial termination

M. Heinemann et al.

Title Page

Abstract

Introduction

Conclusions

References

Tables

Figures

◀

▶

◀

▶

Back

Close

Full Screen / Esc

Printer-friendly Version

Interactive Discussion



## Simulating the last glacial termination

M. Heinemann et al.

Title Page

Abstract

Introduction

Conclusions

References

Tables

Figures

◀

▶

◀

▶

Back

Close

Full Screen / Esc

Printer-friendly Version

Interactive Discussion



time, the Northern Hemisphere ice sheets reach a near-equilibrium volume of about 300 msle and, in contrast to the transient LGM ice sheets in CTR, cover vast areas of northern Asia/Siberia (Fig. 5a). Even for this near-equilibrium state, the ice-sheet is still very dynamic, with long-term variability with negative mass balance terms (ablation, calving, basal melting) of more than 40 msle per thousand years (almost 0.5 Sv) compensating accumulation (Fig. 5c). The simulated North American LGM ice sheet in CTR has a similar extent to that in the fixed LGM boundary condition sensitivity experiment (Fig. 5b), suggesting that the Laurentide ice sheet under LGM conditions in CTR may have been close to its longterm steady state. These results are consistent with previous results by Abe-Ouchi et al. (2013). They illustrated in their Fig. 2b that, during glacial cycles, in insolation/ice volume phase space, the transiently simulated Laurentide ice sheet oscillates much closer to the respective equilibrium solutions than the Eurasian ice sheet.

## 5 Discussion and conclusions

Supporting the astronomical theory of ice ages, the presented model results demonstrate that the initial timing of the last glacial termination was determined by orbitally-induced insolation changes triggering rapid Northern Hemisphere ice sheet retreat shortly after the LGM. This finding is in agreement with recent sea level estimates (Clark et al., 2012), which indicate early meltwater releases around 19 ka BP. However, according to our modeling experiments, orbital forcing alone was not sufficient, and the effects of GHG changes need to be taken into account to explain the fast and full retreat of the North American and Eurasian ice sheets during the deglaciation. These results further emphasize how important it is to identify the mechanisms responsible for the orbital-scale modulation of atmospheric CO<sub>2</sub> concentrations.

The simulated 3 ka lag of the CO<sub>2</sub> increase relative to the onset of the deglaciation should be interpreted with caution, because of the applied acceleration technique. The atmosphere-ocean model is run with orbital and GHG forcing accelerated by a factor of

**Simulating the last glacial termination**

M. Heinemann et al.

[Title Page](#)[Abstract](#)[Introduction](#)[Conclusions](#)[References](#)[Tables](#)[Figures](#)[◀](#)[▶](#)[◀](#)[▶](#)[Back](#)[Close](#)[Full Screen / Esc](#)[Printer-friendly Version](#)[Interactive Discussion](#)

20. For each climate–ice-sheet coupling interval, the atmosphere and ocean only have 50 yr to adjust to the 1000 yr orbital and GHG changes before a new climatology is passed to the ice sheet model. This means that the 3 ka lag is equivalent to only 3 coupling timesteps or 150 atmosphere-ocean years. Without acceleration, the atmosphere and ocean would have more time to adjust to the rising CO<sub>2</sub> during the deglaciation. The ice sheets could hence be affected by the CO<sub>2</sub> rise quicker and stronger, but of course not before the start of the CO<sub>2</sub> rise around 18 kaBP. For the period after 22 kaBP, the composite CO<sub>2</sub> record used here (Lüthi et al., 2008) was based on measured CO<sub>2</sub> concentrations in gas bubbles enclosed in the Antarctic Dome C ice core (Monnin et al., 2001), and the EDC3 gas age chronology (Parrenin et al., 2007). Despite uncertainties in the order of 1 ka with respect to the dating of the CO<sub>2</sub> reconstructions at the onset of the deglaciation (Schwander et al., 2001; Parrenin et al., 2007, 2013; Pedro et al., 2012), the qualitative result that the orbital changes had the potential to, and in our model did in fact initiate the deglaciation holds.

As described in Sect. 2, to account for the low CO<sub>2</sub> sensitivity of LOVECLIM, the effect of CO<sub>2</sub> variations on the longwave flux in the atmosphere is scaled by a factor  $\alpha = 3$ . With this factor, the model best matches the reconstructed deglacial sea level and surface temperature changes (Figs. 2a and 4a). Sensitivity runs with  $\alpha = 2.5$  and  $\alpha = 3.5$  illustrate that the choice of  $\alpha$  has a large effect on the results. The simulated and reconstructed sea level evolutions deviate substantially for both sensitivity runs (Fig. 6), indicating that a realistic glacial cycle can only be achieved within a small range of climate sensitivities. While this scaling factor is not well constrained, the working assumption is that it somewhat mimics the effect of missing feedbacks in the intermediate complexity climate model. For example, clouds are prescribed according to ISCCP D2 (Rossow et al., 1996) in EcBilt. Cloud feedbacks, which potentially amplify the orbital and CO<sub>2</sub> forcing at high latitudes – for instance via the convective cloud feedback (Abbot and Tziperman, 2009) – are neglected. Future simulations with iLove including an empirically derived interactive cloud parameterization (Sriver et al., 2014) are planned.

## Simulating the last glacial termination

M. Heinemann et al.

[Title Page](#)

[Abstract](#)

[Introduction](#)

[Conclusions](#)

[References](#)

[Tables](#)

[Figures](#)

[I ◀](#)

[▶ I](#)

[◀](#)

[▶](#)

[Back](#)

[Close](#)

[Full Screen / Esc](#)

[Printer-friendly Version](#)

[Interactive Discussion](#)



Continental scale ice sheets can largely influence the hydrology over land and water discharge into the ocean. Ice sheet meltwater in form of river runoff or icebergs has long been identified as a potential cause for ocean circulation changes (Stommel, 1961; Ruddiman and McIntyre, 1981). Reconstructions of the deglacial drainage chronology and drainage locations (Tarasov and Peltier, 2006), and atmosphere-ocean model studies (Mikolajewicz et al., 1997; Roche et al., 2009; Liu et al., 2009; Okazaki et al., 2010; Menviel et al., 2011) suggested that meltwater from the Laurentide ice sheet led to reduced North Atlantic deepwater formation after the LGM. The mass balance analysis presented in Sect. 4.3 shows that even before the LGM the large simulated ice sheets are dynamically very active, and characterized by accumulation, and melting/calving on the order of 0.25 Sv (Fig. 2b). The redistribution of freshwater input into the ocean due to the ice sheets may have had a large effect on the ocean circulation even in the absence of a net ice mass loss – for example due to the about 60 % increase in ice sheet calving and related freshwater flux forcing between 28 and 20 kaBP. This effect, however, is not captured by our model simulations, because the ice sheet/ocean freshwater coupling is not activated for the accelerated experiments. Future, unaccelerated runs that include an interactive hydrological model, and capture the meltwater runoff are required to study potential ocean circulation changes and their effect on the deglaciation.

*Acknowledgements.* M. Heinemann was supported by NSF grant #1010869. A. Timmermann and O. E. Timm were supported by the Japan Agency for Marine-Earth Science and Technology (JAMSTEC) through its sponsorship of the International Pacific Research Center.

## References

- Abbot, D. S. and Tziperman, E.: Controls on the activation and strength of a high-latitude convective cloud feedback, *J. Atmos. Sci.*, 66, 519–529, 2009. 520
- Abe-Ouchi, A. and Blatter, H.: On the initiation of ice sheets, *Ann. Glaciol.*, 18, 203–203, 1993. 514

## Simulating the last glacial termination

M. Heinemann et al.

Title Page

Abstract

Introduction

Conclusions

References

Tables

Figures

◀

▶

◀

▶

Back

Close

Full Screen / Esc

Printer-friendly Version

Interactive Discussion



Abe-Ouchi, A., Segawa, T., and Saito, F.: Climatic Conditions for modelling the Northern Hemisphere ice sheets throughout the ice age cycle, *Clim. Past*, 3, 423–438, doi:10.5194/cp-3-423-2007, 2007. 511, 512

Abe-Ouchi, A., Saito, F., Kawamura, K., Raymo, M. E., Okuno, J., Takahashi, K., and Blatter, H.: Insolation-driven 100,000-year glacial cycles and hysteresis of ice-sheet volume, *Nature*, 500, 190–193, 2013. 511, 512, 515, 519

Berger, A. L.: Long-term variations of daily insolation and Quaternary climatic changes, *J. Atmos. Sci.*, 35, 2362–2367, 1978. 510, 512, 528

Brovkin, V., Ganopolski, A., Claussen, M., Kubatzki, C., and Petoukhov, V.: Modelling climate response to historical land cover change, *Global Ecol. Biogeogr.*, 8, 509–517, 1999. 513

Calov, R., Ganopolski, A., Claussen, M., Petoukhov, V., and Greve, R.: Transient simulation of the last glacial inception, Part I: Glacial inception as a bifurcation in the climate system, *Clim. Dynam.*, 24, 545–561, 2005. 514

Clark, P. U., Shakun, J. D., Baker, P. A., Bartlein, P. J., Brewer, S., Brook, E., Carlson, A. E., Cheng, H., Kaufman, D. S., Liu, Z., Marchitto, T. M., Mix, A. C., Morrill, C., Otto-Bliesner, B. L., Pahnke, K., Russell, J. M., Whitlock, C., Adkins, J. F., Blois, J. L., Clark, J., Colman, S. M., Curry, W. B., Flower, B. P., He, F., Johnson, T. C., Lynch-Stieglitz, J., Markgraf, V., McManus, J., Mitrovica, J. X., Moreno, P. I., and Williams, J. W.: Global climate evolution during the last deglaciation, *P. Natl. Acad. Sci. USA*, 109, E1134–E1142, 2012. 510, 519

Driesschaert, E., Fichet, T., Goosse, H., Huybrechts, P., Janssens, I., Mouchet, A., Munhoven, G., Brovkin, V., and Weber, S. L.: Modeling the influence of Greenland ice sheet melting on the Atlantic meridional overturning circulation during the next millennia, *Geophys. Res. Lett.*, 34, L10707, doi:10.1029/2007GL029516, 2007. 512

Gallée, H., van Ypersele, J. P., Fichet, T., Marsiat, I., Tricot, C., and Berger, A.: Simulation of the last glacial cycle by a coupled, sectorially averaged climate-ice sheet model: 2. Response to insolation and CO<sub>2</sub> variations, *J. Geophys. Res.*, 97, 15713–15740, 1992. 510, 511, 517

Ganopolski, A. and Calov, R.: The role of orbital forcing, carbon dioxide and regolith in 100 kyr glacial cycles, *Clim. Past*, 7, 1415–1425, doi:10.5194/cp-7-1415-2011, 2011. 511

Ganopolski, A. and Roche, D. M.: On the nature of lead-lag relationships during glacial-interglacial climate transitions, *Quaternary Sci. Rev.*, 28, 3361–3378, 2009. 511

Gildor, H. and Tziperman, E.: Sea ice as the glacial cycles' climate switch: role of seasonal and orbital forcing, *Paleoceanography*, 15, 605–615, 2000. 511

## Simulating the last glacial termination

M. Heinemann et al.

Title Page

Abstract

Introduction

Conclusions

References

Tables

Figures

◀

▶

◀

▶

Back

Close

Full Screen / Esc

Printer-friendly Version

Interactive Discussion



- Goosse, H. and Fichefet, T.: Importance of ice-ocean interactions for the global ocean circulation: a model study, *J. Geophys. Res.-Sol. Ea.*, 104, 23337–23355, 1999. 513
- Goosse, H., Brovkin, V., Fichefet, T., Haarsma, R., Huybrechts, P., Jongma, J., Mouchet, A., Seltén, F., Barriat, P.-Y., Campin, J.-M., Deleersnijder, E., Driesschaert, E., Goelzer, H., Janssens, I., Loutre, M.-F., Morales Maqueda, M. A., Opsteegh, T., Mathieu, P.-P., Munhoven, G., Pettersson, E. J., Renssen, H., Roche, D. M., Schaeffer, M., Tartinville, B., Timmermann, A., and Weber, S. L.: Description of the Earth system model of intermediate complexity LOVECLIM version 1.2, *Geosci. Model Dev.*, 3, 603–633, doi:10.5194/gmd-3-603-2010, 2010. 512
- Gregoire, L. J., Payne, A. J., and Valdes, P. J.: Deglacial rapid sea level rises caused by ice-sheet saddle collapses, *Nature*, 487, 219–222, 2012. 515
- He, F., Shakun, J. D., Clark, P. U., Carlson, A. E., Liu, Z., Otto-Bliesner, B. L., and Kutzbach, J. E.: Northern Hemisphere forcing of Southern Hemisphere climate during the last deglaciation, *Nature*, 494, 81–85, 2013. 511
- Jones, P. D. and Moberg, A.: Hemispheric and large-scale surface air temperature variations: an extensive revision and an update to 2001, *J. Climate*, 16, 206–223, 2003. 527
- Källén, E., Crafoord, C., and Ghil, M.: Free oscillations in a climate model with ice-sheet dynamics, *J. Atmos. Sci.*, 36, 2292–2303, 1979. 511
- Liu, Z., Otto-Bliesner, B. L., He, F., Brady, E. C., Tomas, R., Clark, P. U., Carlson, A. E., Lynch-Stieglitz, J., Curry, W., Brook, E., Erickson, D., Jacob, R., Kutzbach, J., and Cheng, J.: Transient simulation of last deglaciation with a new mechanism for Bolling–Allerod warming, *Science*, 325, 310–314, 2009. 521
- Loulergue, L., Schilt, A., Spahni, R., Masson-Delmotte, V., Blunier, T., Lemieux, B., Barnola, J.-M., Raynaud, D., Stocker, T. F., and Chappellaz, J.: Orbital and millennial-scale features of atmospheric CH<sub>4</sub> over the past 800,000 years, *Nature*, 453, 383–386, 2008. 512
- Lüthi, D., Le Floch, M., Bereiter, B., Blunier, T., Barnola, J.-M., Siegenthaler, U., Raynaud, D., Jouzel, J., Fischer, H., Kawamura, K., and Stocker, T. F.: High-resolution carbon dioxide concentration record 650,000–800,000 years before present, *Nature*, 453, 379–382, 2008. 512, 520, 528
- Marcott, S. A., Shakun, J. D., Clark, P. U., and Mix, A. C.: A Reconstruction of Regional and Global Temperature for the Past 11 300 Years, *Science*, 339, 1198–1201, 2013. 518, 530

## Simulating the last glacial termination

M. Heinemann et al.

Title Page

Abstract

Introduction

Conclusions

References

Tables

Figures

◀

▶

◀

▶

Back

Close

Full Screen / Esc

Printer-friendly Version

Interactive Discussion



- Menviel, L., Timmermann, A., and Timm, O. E.: Deconstructing the Last Glacial termination: the role of millennial and orbital-scale forcings, *Quaternary Sci. Rev.*, 30, 1155–1172, 2011. 521
- Mikolajewicz, U., Crowley, T. J., Schiller, A., and Voss, R.: Modelling teleconnections between the North Atlantic and North Pacific during the Younger Dryas, *Nature*, 387, 384–387, 1997. 521
- Milankovitch, M.: *Kanon der Erdebestrahlung und seine Anwendung auf das Eiszeitenproblem*, Königlich Serbische Akademie, Belgrad, 1941. 510
- Monnin, E., Indermühle, A., Dällenbach, A., Flückiger, J., Stauffer, B., Stocker, T. F., Raynaud, D., and Barnola, J.-M.: Atmospheric CO<sub>2</sub> concentrations over the last glacial termination, *Science*, 291, 112–114, 2001. 520
- Okazaki, Y., Timmermann, A., Menviel, L., Harada, N., Abe-Ouchi, A., Chikamoto, M. O., Mouchet, A., and Asahi, H.: Deepwater formation in the North Pacific during the last glacial termination, *Science*, 329, 200–204, 2010. 521
- Opsteegh, J. D., Haarsma, R. J., Selten, F. M., and Kattenberg, A.: ECBILT: a dynamic alternative to mixed boundary conditions in ocean models, *Tellus A*, 50, 348–367, 1998. 512
- Parrenin, F., Barnola, J.-M., Beer, J., Blunier, T., Castellano, E., Chappellaz, J., Dreyfus, G., Fischer, H., Fujita, S., Jouzel, J., Kawamura, K., Lemieux-Dudon, B., Loulergue, L., Masson-Delmotte, V., Narcisi, B., Petit, J.-R., Raisbeck, G., Raynaud, D., Ruth, U., Schwander, J., Severi, M., Spahni, R., Steffensen, J. P., Svensson, A., Udisti, R., Waelbroeck, C., and Wolff, E.: The EDC3 chronology for the EPICA Dome C ice core, *Clim. Past*, 3, 485–497, doi:10.5194/cp-3-485-2007, 2007. 520
- Parrenin, F., Masson-Delmotte, V., Kohler, P., Raynaud, D., Paillard, D., Schwander, J., Barbante, C., Landais, A., Wegner, A., and Jouzel, J.: Synchronous change of atmospheric CO<sub>2</sub> and Antarctic temperature during the last deglacial warming, *Science*, 339, 1060–1063, 2013. 520
- Pedro, J. B., Rasmussen, S. O., and van Ommen, T. D.: Tightened constraints on the time-lag between Antarctic temperature and CO<sub>2</sub> during the last deglaciation, *Clim. Past*, 8, 1213–1221, doi:10.5194/cp-8-1213-2012, 2012. 520
- Peltier, W. R.: Global glacial isostasy and the surface of the ice-age earth: the ICE5G (VM2) model and grace, *Annu. Rev. Earth Planet. Sci.*, 32, 111–149, 2004. 515, 528, 529

## Simulating the last glacial termination

M. Heinemann et al.

Title Page

Abstract

Introduction

Conclusions

References

Tables

Figures

◀

▶

◀

▶

Back

Close

Full Screen / Esc

Printer-friendly Version

Interactive Discussion



- Peltier, W. R. and Fairbanks, R. G.: Global glacial ice volume and Last Glacial Maximum duration from an extended Barbados sea level record, *Quaternary Sci. Rev.*, 25, 3322–3337, 2006. 510, 528
- Pollard, D. and Thompson, S. L.: Driving a high-resolution dynamic ice-sheet model with GeM climate: ice-sheet initiation at 116 000 BP, *Ann. Glaciol.*, 25, 296–304, 1997. 514
- Roche, D. M., Wiersma, A. P., and Renssen, H.: A systematic study of the impact of freshwater pulses with respect to different geographical locations, *Clim. Dynam.*, 34, 997–1013, 2009. 521
- Roche, D. M., Renssen, H., Paillard, D., and Levvasseur, G.: Deciphering the spatio-temporal complexity of climate change of the last deglaciation: a model analysis, *Clim. Past*, 7, 591–602, doi:10.5194/cp-7-591-2011, 2011. 511
- Roe, G. H. and Lindzen, R. S.: The mutual interaction between continental-scale ice sheets and atmospheric stationary waves, *J. Climate*, 14, 1450–1465, 2001. 511
- Rossov, W. B., Walker, A. W., Beuschel, D., and Roiter, M.: International Satellite Cloud Climatology Project (ISSCP) Description of New Cloud Datasets, WMO/TD 737, World Climate Research Programme (ICSU and WMO), <http://www.cgd.ucar.edu/cas/catalog/satellite/isccp/D2/references.html>, last access: February 2014, 115 pp., 1996. 520
- Ruddiman, W. F. and McIntyre, A.: The North Atlantic Ocean during the last deglaciation, *Palaeogeogr. Palaeoclimatol.*, 35, 145–214, 1981. 521
- Saito, F. and Abe-Ouchi, A.: Thermal structure of Dome Fuji and east Dronning Maud Land, Antarctica, simulated by a three-dimensional ice-sheet model, *Ann. Glaciol.*, 39, 433–438, 2004. 512
- Schaeffer, M., Selten, F., and van Dortland, R.: Linking IMAGE and ECBILT, Tech. Rep. 481508008, National Institute for public health and the environment (RIVM), Bilthoven, the Netherlands, 1999. 512
- Schilt, A., Baumgartner, M., Blunier, T., Schwander, J., Spahni, R., Fischer, H., and Stocker, T. F.: Glacial-interglacial and millennial-scale variations in the atmospheric nitrous oxide concentration during the last 800,000 years, *Quaternary Sci. Rev.*, 29, 182–192, 2010. 512
- Schwander, J., Jouzel, J., Hammer, C. U., Petit, J.-R., Udisti, R., and Wolff, E.: A tentative chronology for the EPICA Dome Concordia Ice Core, *Geophys. Res. Lett.*, 28, 4243–4246, 2001. 520

## Simulating the last glacial termination

M. Heinemann et al.

Title Page

Abstract

Introduction

Conclusions

References

Tables

Figures

◀

▶

◀

▶

Back

Close

Full Screen / Esc

Printer-friendly Version

Interactive Discussion



- Shakun, J. D., Clark, P. U., He, F., Marcott, S. A., Mix, A. C., Liu, Z., Otto-Bliesner, B., Schmit-  
tner, A., and Bard, E.: Global warming preceded by increasing carbon dioxide concentrations  
during the last deglaciation, *Nature*, 484, 49–55, 2012. 510, 518, 530
- Smith, R. S. and Gregory, J.: The last glacial cycle: transient simulations with an AOGCM, *Clim.*  
*Dynam.*, 38, 1545–1559, 2012. 511
- 5 Sriver, R. L., Timmermann, A., Mann, M. E., Keller, K., and Goosse, H.: Improved represen-  
tation of tropical Pacific ocean-atmosphere dynamics in an intermediate complexity climate  
model, *J. Climate*, 27, 168–185, 2014. 520
- Stommel, H.: Thermohaline convection with two stable regimes of flow, *Tellus*, 13, 224–230,  
10 1961. 521
- Tarasov, L. and Peltier, W. R.: A calibrated deglacial drainage chronology for the North American  
continent: evidence of an Arctic trigger for the Younger Dryas, *Quaternary Sci. Rev.*, 25, 659–  
688, 2006. 521
- Timm, O. and Timmermann, A.: Simulation of the last 21 000 years using accelerated transient  
15 boundary conditions, *J. Climate*, 20, 4377–4401, 2007. 511, 513
- Timmermann, A., Timm, O., Stott, L., and Menviel, L.: The Roles of CO<sub>2</sub> and orbital forcing in  
driving southern hemispheric temperature variations during the last 21 000 yr, *J. Climate*, 22,  
1626–1640, 2009. 511
- 20 Waelbroeck, C., Labeyrie, L., Michel, E., Duplessy, J. C., McManus, J. F., Lambeck, K., Bal-  
bon, E., and Labracherie, M.: Sea-level and deep water temperature changes derived from  
benthic foraminifera isotopic records, *Quaternary Sci. Rev.*, 21, 295–305, 2002. 510, 514,  
527, 528, 531, 532
- Yamagishi, T., Abe-Ouchi, A., Saito, F., Segawa, T., and Nishimura, T.: Re-evaluation of paleo-  
accumulation parameterization over Northern Hemisphere ice sheets during the ice age ex-  
25 amined with a high-resolution AGCM and a 3-D ice-sheet model, *Ann. Glaciol.*, 42, 433–440,  
2005. 511
- Yokoyama, Y. and Esat, T. M.: Global climate and sea level: enduring variability and rapid fluc-  
tuations over the past 150 000 years, *Oceanography*, 24, 54–69, 2011. 510, 515, 528
- 30 Yoshimori, M., Weaver, A. J., Marshall, S. J., and Clarke, G. K. C.: Glacial termination: sensitivity  
to orbital and CO<sub>2</sub> forcing in a coupled climate system model, *Clim. Dynam.*, 17, 571–588–  
588, 2001. 511, 517

## Simulating the last glacial termination

M. Heinemann et al.

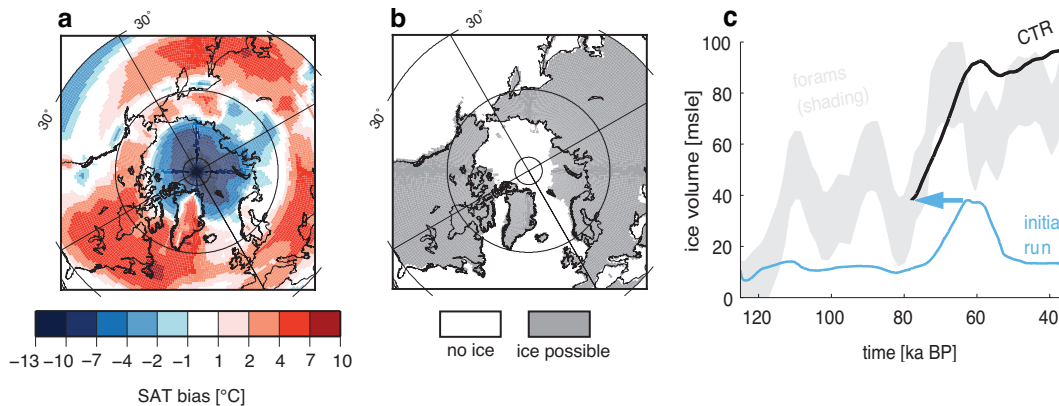


**Fig. 1.** Model setup and initialization. **(a)** LOVECLIM surface air temperature (SAT) bias computed from annual mean 2 m air temperature from a LOVECLIM present-day simulation with prescribed ICE-5G ice sheets minus a 1960 to 1990 annual mean surface air temperature climatology derived from observations (Jones and Moberg, 2003). **(b)** IclES grounding line. The effect of sea level and bedrock elevation changes, as well as variable ice shelves on the ice sheet grounding line are neglected in the IclES model setup used here. The grounding line is fixed, ice sheets can only grow within the gray-shaded area. **(c)** Ice sheet initialization. Using the standard iLove coupled model initialized at the Eemian (125 kaBP), a glacial inception with a magnitude comparable to reconstructions (Waelbroeck et al., 2002, gray shading) only sets in around 70 kaBP (blue line, initial run). The blue arrow illustrates the second step as described in the text, restarting the simulation at 78 kaBP with initial conditions from the blue run at 63 kaBP. The re-initialized run (black line) is used as the control run (CTR) in the present study.

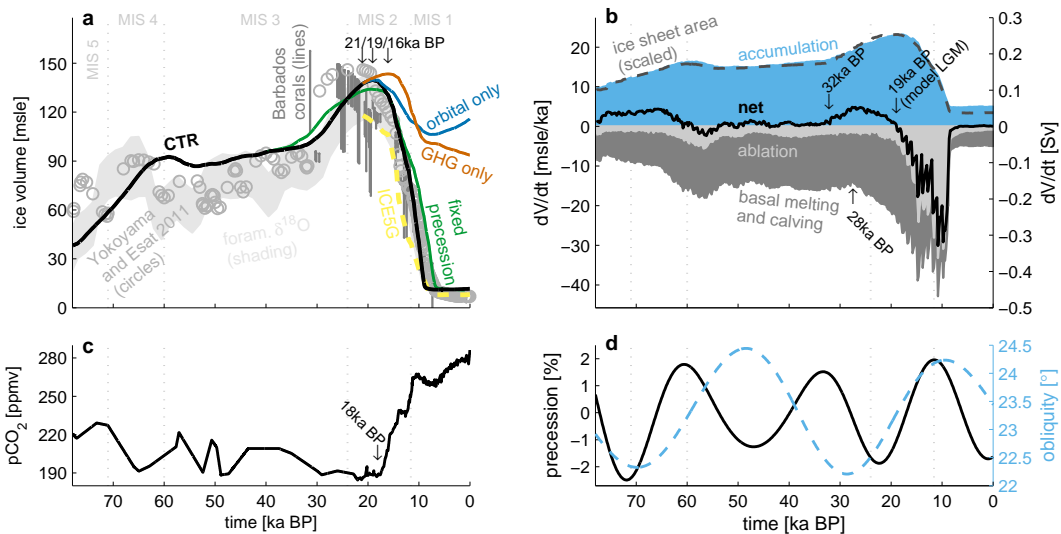


**Fig. 2.** Ice sheet evolution, mass balance, and drivers. **(a)** Simulated NH ice sheet volume in meters sea level equivalent (m sle) from control run with both orbital and GHG forcing (CTR, thick black), only GHG forcing (orange, fixed 21 ka BP orbit), and only orbital forcing (blue, fixed 21 ka BP GHGs). Reconstructed NH ice volume (Peltier, 2004, ICE-5G, yellow dashed line), and reconstructed global sea level changes from Barbados coral record (Peltier and Fairbanks, 2006, vertical gray lines), from foraminiferal records (Waelbroeck et al., 2002, light gray shading), and from coral terraces at Huon Peninsula, Papua New Guinea (Yokoyama and Esat, 2011, gray circles). **(b)** Ice volume rate of change due to accumulation (blue area), ablation (light gray area), basal melting and calving (dark gray area), and their balance (net, thick black line) from CTR. Dashed gray line indicates the simulated NH ice sheet area scaled by  $\max(\text{accumulation})/\max(\text{area})$ . **(c)**  $CO_2$  forcing (Lüthi et al., 2008). **(d)** Precessional index (black line, high values indicate NH summers closer to the sun), and obliquity (Berger, 1978, dashed blue line). The dotted gray vertical lines indicate boundaries between marine isotope stages (MIS).

## Simulating the last glacial termination

M. Heinemann et al.

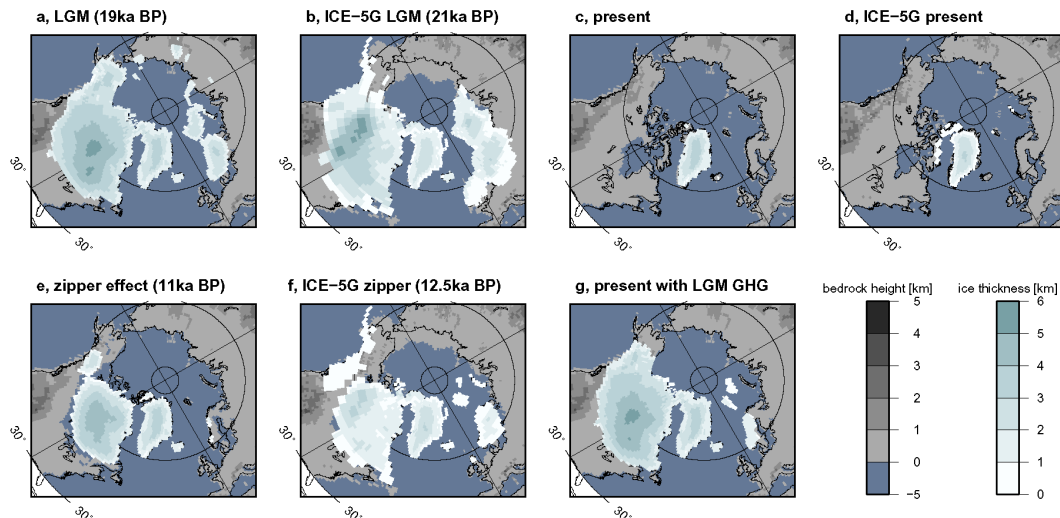


**Fig. 3.** Bedrock height and ice sheet thickness **(a)** at the Last Glacial Maximum (LGM) as simulated with iLove, **(b)** at the LGM according to the ICE-5G reconstruction (Peltier, 2004), **(c)** at present (0 kaBP) as simulated with iLove, **(d)** at present according to ICE-5G, **(e)** at 11 kaBP, which is when the Cordilleran and Labrador ice sheets separate in iLove (zipper effect), **(f)** zipper effect for the ICE-5G reconstructions at 12.5 kaBP, and **(g)** as simulated for the present (0 kaBP), assuming that atmospheric greenhouse gases (GHGs) remained constant at their LGM values (21 kaBP). Black contours show observed present-day coastlines for reference.

Title Page

Abstract

Introduction

Conclusions

References

Tables

Figures

◀

▶

◀

▶

Back

Close

Full Screen / Esc

Printer-friendly Version

Interactive Discussion



## Simulating the last glacial termination

M. Heinemann et al.

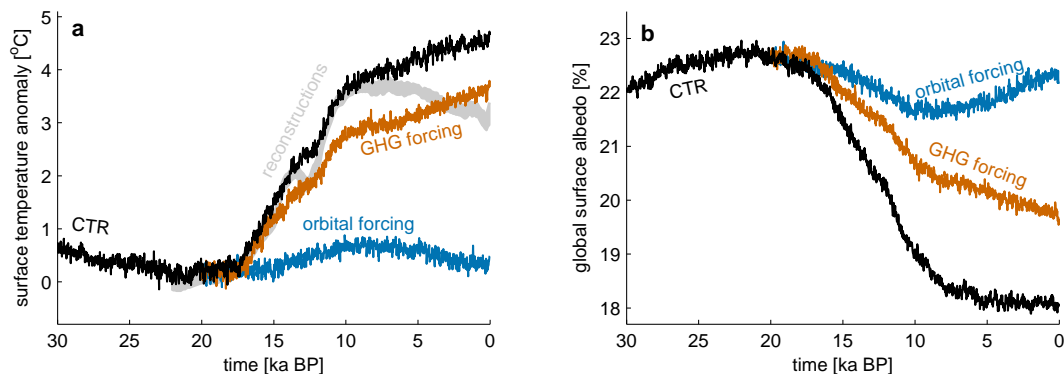


**Fig. 4.** Evolution of global mean annual mean surface temperature anomaly relative to 21 kaBP (**a**), and surface albedo (**b**), for the control run with both orbital and GHG forcing (black, CTR), only GHG forcing (orange, fixed 21 kaBP orbit), and only orbital forcing (blue, fixed 21 kaBP GHGs). Gray shading in panel a shows the reconstructed global mean surface temperature anomaly (Shakun et al., 2012; Marcott et al., 2013).

Title Page

Abstract

Introduction

Conclusions

References

Tables

Figures

◀

▶

◀

▶

Back

Close

Full Screen / Esc

Printer-friendly Version

Interactive Discussion



## Simulating the last glacial termination

M. Heinemann et al.

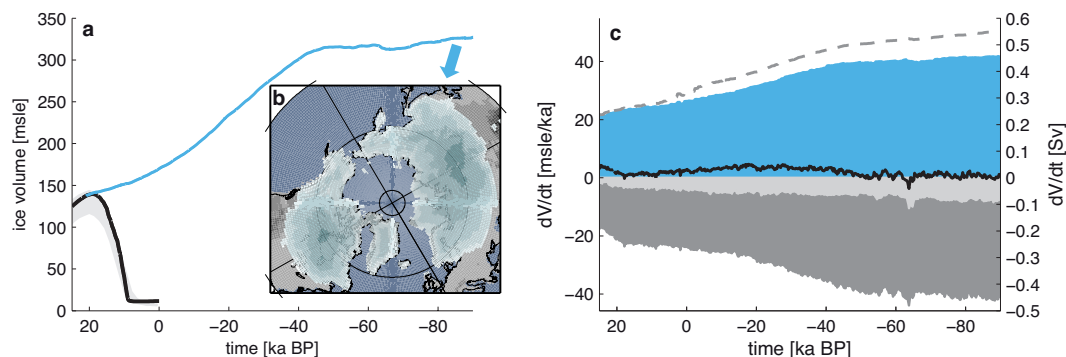


**Fig. 5.** (a) Northern Hemisphere ice sheet volume in meters sea level equivalent (msle) for CTR (black), and for fixed LGM (21 kaBP) greenhouse gas concentrations and orbital parameters (blue line); gray shading indicates sea level reconstructions (Waelbroeck et al., 2002). (b) Bedrock height and ice sheet thickness at -90 kaBP (see Fig. 3 for color scales). (c) Accumulation (blue area), ablation (light gray shading), basal melting and calving (dark gray shading), net mass balance (thick black line), and ice sheet area for comparison (dashed line) scaled as in Fig. 2b.

Title Page

Abstract

Introduction

Conclusions

References

Tables

Figures

◀

▶

◀

▶

Back

Close

Full Screen / Esc

Printer-friendly Version

Interactive Discussion



## Simulating the last glacial termination

M. Heinemann et al.

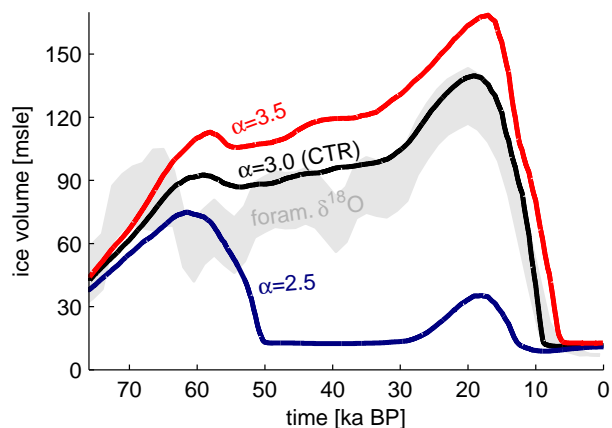


**Fig. 6.** Sensitivity of the simulated Northern Hemisphere land ice volume to the parameter  $\alpha$ , which scales the effect of  $\text{CO}_2$  on the longwave radiation in the atmosphere (Sect. 2). The default value as used in this study is  $\alpha = 3$  (CTR). Gray shading indicates sea level reconstructions from foraminiferal oxygen isotope ratios (Waelbroeck et al., 2002).

[Title Page](#)[Abstract](#)[Introduction](#)[Conclusions](#)[References](#)[Tables](#)[Figures](#)[I◀](#)[▶I](#)[◀](#)[▶](#)[Back](#)[Close](#)[Full Screen / Esc](#)[Printer-friendly Version](#)[Interactive Discussion](#)